Enclosure 1: #65

SANDIA REPORT
SAND86—1916
Internal Distribution Only
Printed April 1987

Analyses of the ASP Test Vehicle Recovery System

D. W. Kuntz

Prepared by
Sandia National Laboratories
Albuquerque, New Mexico 87185 and Livermore, California 94550
for the United States Department of Energy
under Contract DE-AC04-76DP00789

Issued by Sandia National Laboratories, operated for the United States Department of Energy by Sandia Corporation.

Contents

Figures

Analyses of the ASP Test Vehicle Recovery System

1. Introduction

The Anti-Submarine Penetrator (ASP) test vehicle contains a recovery system designed to return the vehicle to the ocean surface upon completion of the water-entry portion of the test flight. The recovery system, designed by D. W. Johnson of Division 1552, is deployed after the vehicle has entered the water and decelerated to its terminal sink rate. The system consists of a 4.1-ft diameter Kevlar ribbon parachute, a Kevlar flotation bag, a urethane-coated nylon flotation bag liner, and a gas generator built by Rocket Research Corporation (RRC). The parachute is intended to slow the vehicle from its 50 to 55 ft/s terminal velocity to approximately 10 ft/s while the gas generator inflates the flotation bag liner. The buoyant force produced by the gas is then transmitted through the Kevlar flotation bag to the vehicle, returning the assembly to the surface. The gases used to inflate the flotation bag result from mixing the combustion products of solid rocket fuel with carbon-dioxide. The gas within the flotation bag is at an elevated temperature immediately after bag deployment. Thus the possibility exists that heat transfer from the gas through the bag assembly to the surrounding seawater could result in a loss of buoyancy and a subsequent loss of the test vehicle. To determine the effects of heat transfer on the performance of the recovery system, an analysis was performed that modeled the dynamics and thermodynamics of the ASP vehicle and its recovery system. The first section of this report presents the details of this analysis and provides performance predictions for the ASP recovery system.

Tests were conducted at Lake Pend Oreille, Idaho, prior to flight testing the vehicle to confirm the performance of the recovery system under actual operating conditions. During one of these tests, the vehicle reached the surface at a relatively high rate of speed, with a large amount of the flotation bag rising above the surface. The vehicle then sank below the surface of the lake, and continued to sink until restrained by a line that had been attached to the nose of the vehicle. Upon retrieving the vehicle with the line, the gas in the flotation bag was found to have sufficient buoyancy to enable the system to float with a relatively small amount of the flotation bag above the surface. To determine the cause of this behavior and to obtain information useful for preventing this phenomenon during the recovery of the flight vehicle, an analysis was performed of the surface arrival of the ASP vehicle. This analysis uses many of the same relations used in the analysis of the recovery system, and thus a description of it is included in the second section of this report.

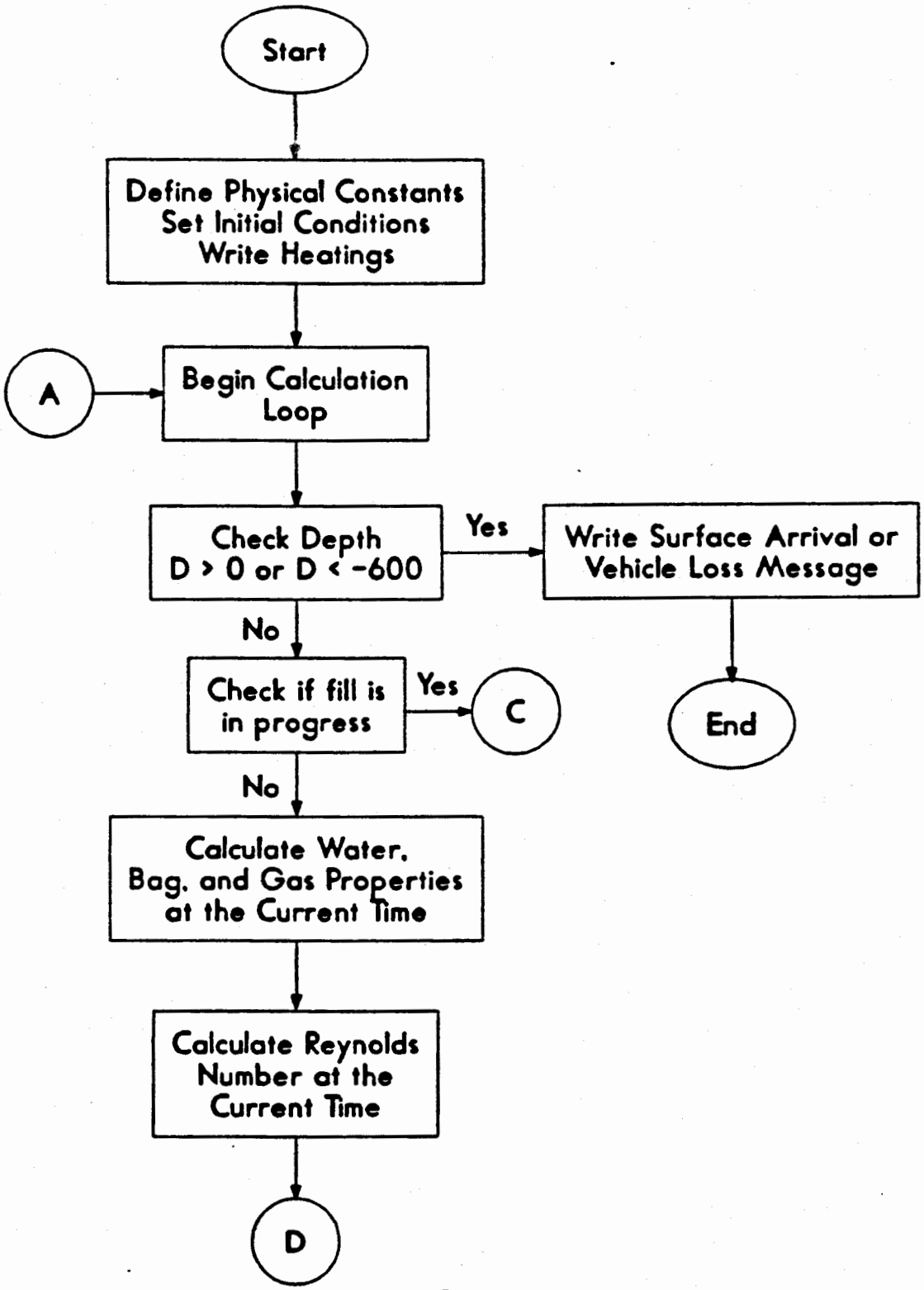

Figure 1. Flow Chart for the Program PENREC

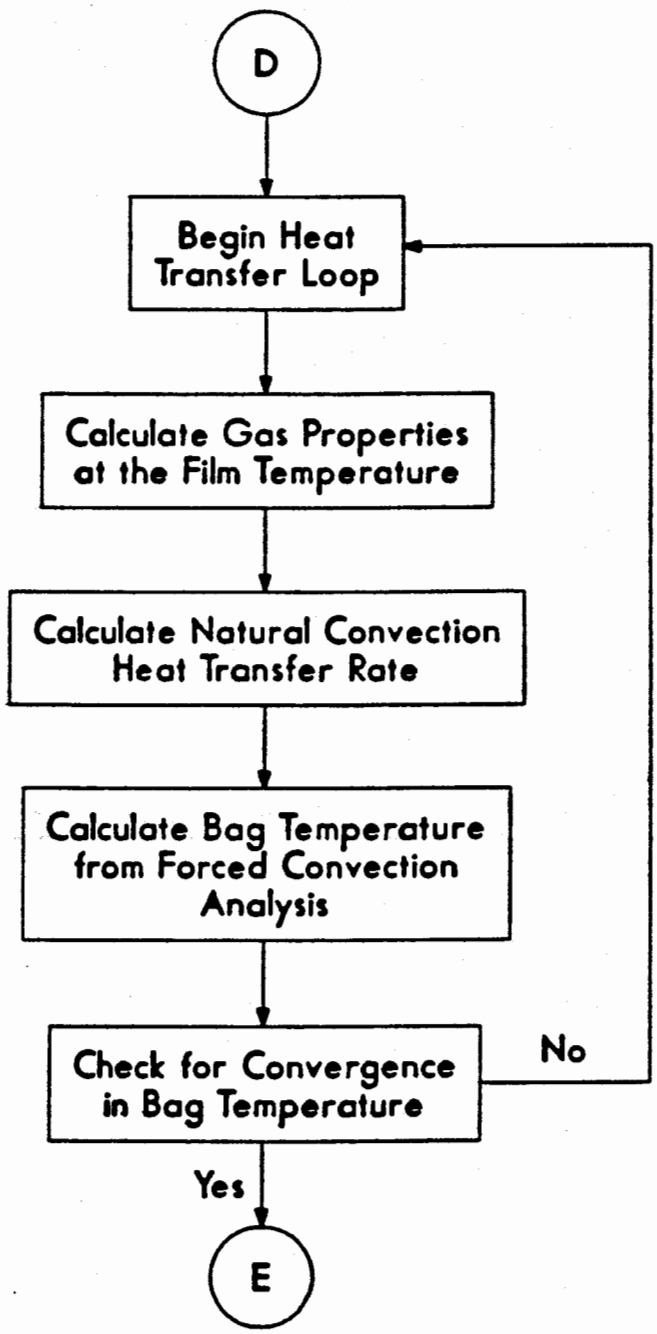

Figure 1. (Continued)

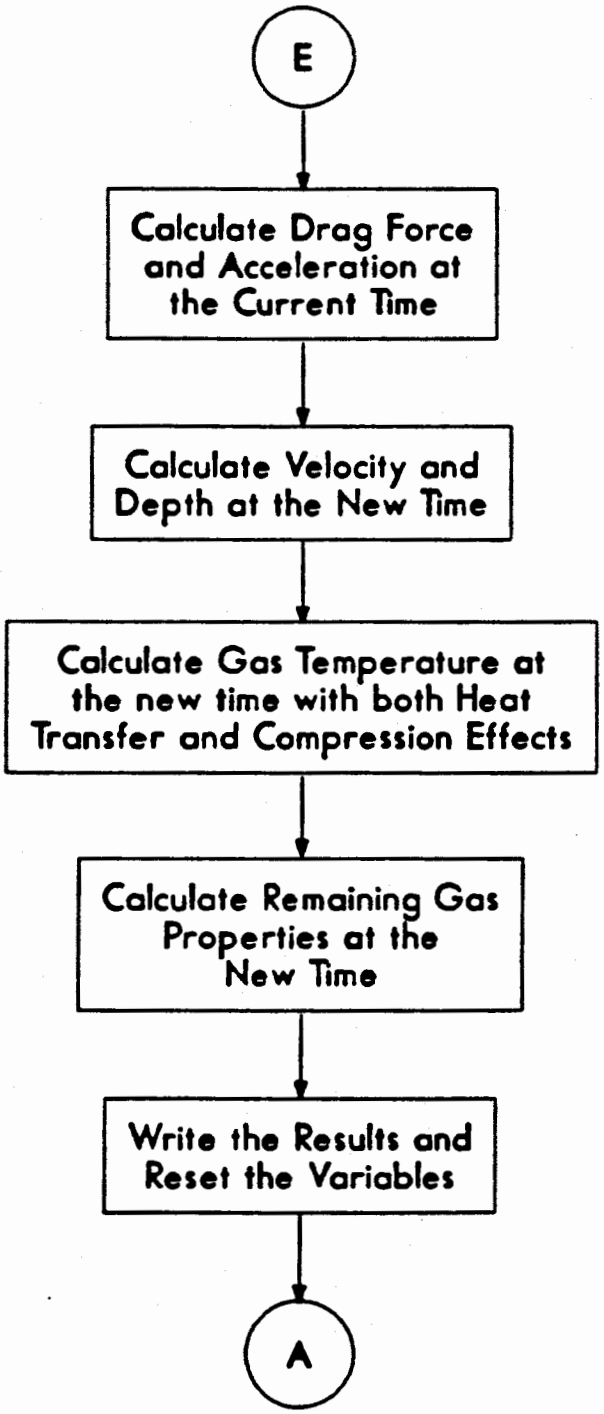

Figure 1. (Continued)

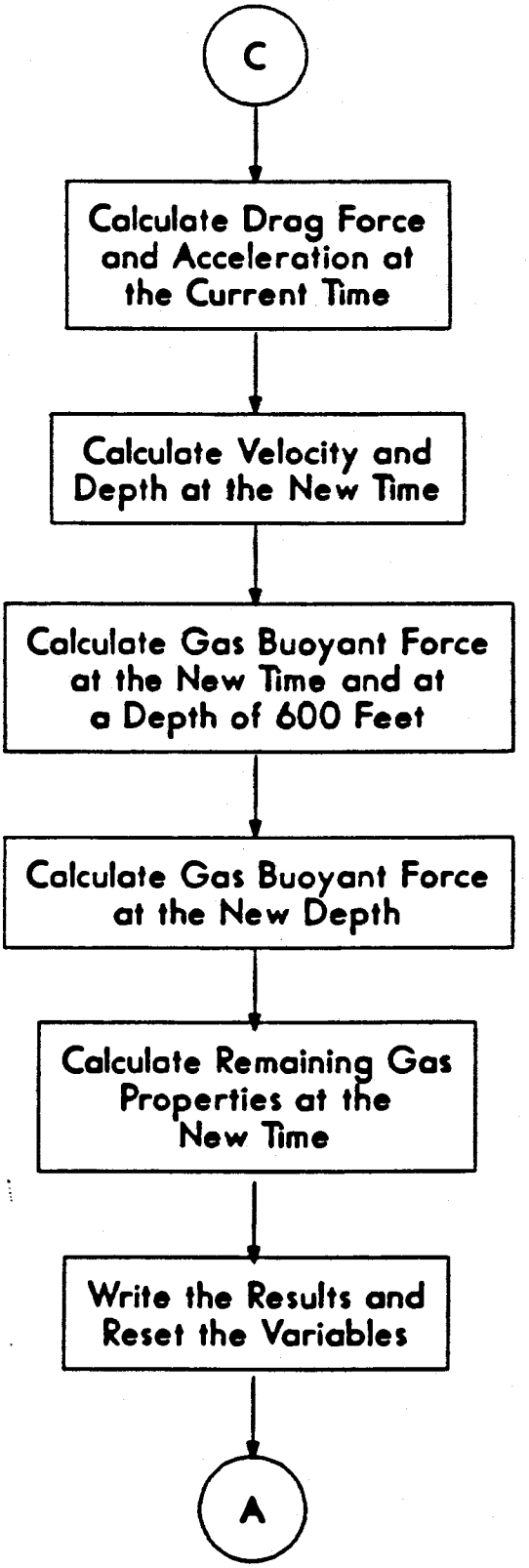

Figure 1. (Concluded)

Governing Equations

The equations used to model the physics of the ASP recovery system are included and described in this subsection. Figure 2 illustrates the coordinate system and some of the variable names used in this analysis.

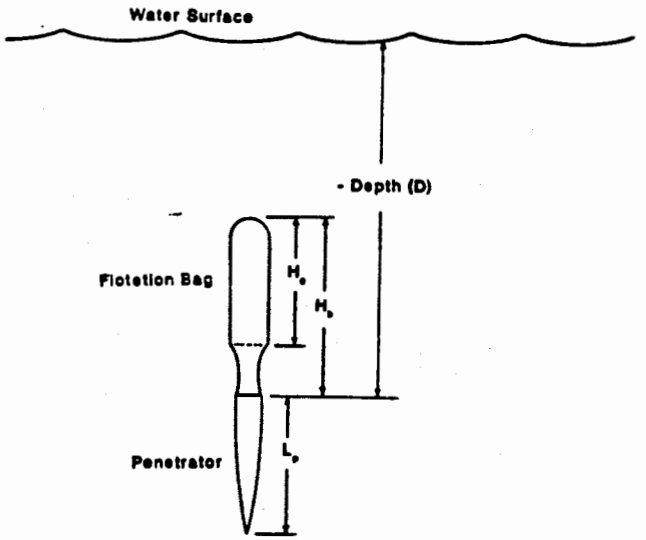

Figure 2. ASP Coordinate System and Variable Names (Parachutes Not Shown)

Vehicle Dynamics

The drag force on the vehicle is calculated from the relation

$$F_d = -\frac{1}{2}C_d\left[\pi\left(\frac{d_b}{2}\right)^2\right]\rho_w|V|V \tag{1}$$

which is derived from the definition of the drag coefficient.

The acceleration of the vehicle is determined from Newton's second law in the form

$$\frac{dV}{dt} = \frac{-W_p + BF_g + BF_p + F_d}{M_p} \tag{2}$$

where the numerator on the right side is simply the sum of the forces acting on the vehicle, and the denominator is the mass of the vehicle.

The velocity at time 2 is determined from the vehicle properties at time 1 with the equation

$$V_2 = \Delta t\left[\frac{dV}{dt}\right]_1 + V_1 \tag{3}$$

and the depth at time 2 is calculated with an average of the velocities at time 2 and time 1 with the equation

$$D_2 = D_1 + \left[\frac{V_1 + V_2}{2}\right]\Delta t\,. \tag{4}$$

Heat Transfer

The natural convection heat transfer from the gas to the flotation bag was calculated with the empirical correlation

$$Nu_{f,nc} = 0.55\,[Gr_f Pr_f]^{0.25} \tag{5}$$

where the Nusselt and Grashof numbers are defined as

$$Nu_{f,nc} = \frac{h_{nc}d_b}{k_f} \tag{6}$$

and

$$Gr_f = \frac{g|T_g - T_b|H_g^3\rho_f^2}{T_g\mu_f^2} \tag{7}$$

and the subscript f means the property of the gas is evaluated at the film temperature, which is the average of the bag and the gas temperatures. This correlation was obtained from studies of transient natural convection in closed vertical cylindrical enclosures.[1]

The heat transfer was then calculated from the relation

$$\dot{Q} = h_{nc}A_g(T_b - T_g)\,. \tag{8}$$

The forced convection heat transfer from the bag to the surrounding seawater is dependent upon whether the flow is laminar or turbulent, and whether the velocity is positive (vehicle moving upward) or negative (vehicle moving downward). The correlations used are based upon flat-plate boundary layer theory with transition occurring at a critical Reynolds number based on length of 5×10^5.

The Reynolds number used to determine transition is based upon total vehicle (penetrator and flotation bag) length for negative velocities, and based upon the height of the gas column within the flotation bag for positive velocities. Thus, the Reynolds number is calculated with the relation

$$Re = \frac{\rho_w|V|(L_p + H_b)}{\mu_w} \tag{9}$$

The gas properties calculated after the completion of the fill process must include the effects of both compression and expansion due to depth change and heat transfer. Initially the pressure, density, and mass of the flotation gas at the current time are calculated with the relations

$$P_g = -D\rho_w g + P_{atm} \tag{21}$$

$$\rho_g = \frac{P_g}{R_g T_g} \tag{22}$$

and

$$M_g = \rho_g \mathcal{V}_g . \tag{23}$$

After completion of the heat-transfer loop and the vehicle dynamics calculations to determine the new depth, the new pressure is calculated with the equation

$$P_{g,2} = -D_2\rho_w g + P_{atm} \tag{24}$$

and the new temperature is calculated in a two step process with the equations

$$T_{g,1a} = \frac{\dot{Q}\Delta t}{M_g C_{Pg}} + T_{g,1} \tag{25}$$

and

$$T_{g,2} = T_{g,1a}\left[\frac{P_{g,2}}{P_{g,1}}\right]^{\frac{\gamma-1}{\gamma}} . \tag{26}$$

Equation 25 is based on the conservation of energy and accounts for the rise in the gas temperature as a result of the heat transfer, and Equation 26 varies the temperature of the gas to account for the isentropic compression or expansion that occurs as the vehicle changes depth. With the new gas temperature known, the new gas volume can be calculated with the ideal gas law

$$\mathcal{V}_{g,2} = \frac{M_g R_g T_{g,2}}{P_{g,2}} . \tag{27}$$

The new gas volume is compared with the maximum gas volume and limited to that amount. A new M_g is calculated using the maximum gas volume if the calculated $\mathcal{V}_g$ was found to exceed the maximum value.

After the calculation of the new gas volume, the new gas buoyant force is calculated with the equation

$$BF_{g,2} = \rho_w g \mathcal{V}_{g,2} . \tag{28}$$

Analysis Results

Nominal Case

The program PENREC was initially run with characteristics and initial conditions consistent with the expected ASP test conditions to ensure that, under nominal operating conditions, the recovery system would return the vehicle to the surface. The ASP vehicle is 65.4 in. long and weighs 803 lbf. The buoyant force of the vehicle used in the analysis was 138 lbf, yielding a submerged weight of 665 lbf. The drag coefficient for the vehicle with a positive velocity was assumed to be 3.824, using the frontal area of the 1.5-ft-diameter flotation bag as the area in the drag equation. This drag coefficient was chosen because it gave a terminal upward velocity of 5 ft/s with a full flotation bag. A more detailed discussion of the positive vertical velocity and its impact on the recovery process will be presented in the second section of this report. The product of the drag coefficient and parachute area for negative velocity conditions was 7 ft^2. This value is based upon the design of the ribbon parachute, which slows the vehicle during the flotation system deployment.

The flotation bag has a height of 92 in. and a diameter of 18 in. A maximum buoyant force of 833.3 lbf from the gas is possible with the 13 ft^3 volume of the bag. The flotation gas was assumed to behave similar to carbon dioxide with a gamma of 1.3 and a gas constant of 35.12 (ft-lbf/lbm-R). The seawater density used was 64.1 (lbm-ft^3) and the ocean temperature was assumed to be 40°F below 600 ft and vary linearly from 40°F to 70°F at depths from 600 ft to the surface. The initial depth of the ASP vehicle was assumed to be 450 ft and the initial velocity was assumed to be 60 ft/s downward. A time-step increment of 0.01 s was used in the calculations. This value is considered sufficiently small relative to the other time scales within this problem to make Equation 3 a reasonably accurate representation of the true vehicle performance.

The results of this analysis using the nominal ASP flight conditions are illustrated in Figures 3, 4, 5, and 6, which are plots of depth, velocity, temperature, and gas buoyant force as functions of time, respectively. An abbreviated program output for this case is presented as a sample output in Appendix B. For this set of input conditions, the ASP vehicle reaches a maximum depth of approximately 480 ft at a time of 4.1 s after the beginning of the recovery sequence. The maximum buoyancy of 833.3 lbf is reached at 5.5 s, and the terminal upward velocity of 5 ft/s is reached at a time of 8.0 s. The cooling of the gas due to the effects of heat transfer and expansion is never large enough to cause the buoyancy to drop below its maximum value. The gas temperature drops to a value equal to the local water temperature at a time of approximately 50 s and continues to drop below the water temperature as the vehicle rises. This indicates that, after this point, the cooling of the gas due to expansion dominates over the heating of the gas by the surrounding seawater. The bag temperature never deviates from the water temperature by more than 5°F, indicating that the forced convection analysis may not have been necessary and that the assumption that the bag temperature equalled the water temperature would have been valid for the nominal case. The vehicle arrives at the surface 100.9 s after initiating the recovery sequence without the buoyancy ever dropping below the maximum value.

Sensitivity Analysis

The analysis of the ASP recovery system indicated that, in the nominal case, the vehicle would return to the surface without loss of buoyancy due to heat-transfer effects. To determine what factors of safety were built into the recovery system, a sensitivity analysis was conducted to learn how much various initial conditions and operating characteristics could be altered without losing the vehicle. This sensitivity analysis is also useful for obtaining a feeling for the quality of the answers produced by the analysis. If the sensitivity analysis indicated that the recovery system was marginal, then the quality of the assumptions made in the analysis could significantly affect the results. However, if the recovery system was found to be tolerant of significant changes in the various initial conditions and operating characteristics, then small inaccuracies in the correlations and assumptions used in the analysis would not be expected to affect the prediction of a successful vehicle recovery.

The calculations within the analysis in which the author has the least amount of confidence are the heat-transfer calculations. The expression for the natural convection within the flotation bag is based upon experimental studies made using vertical cylinders. The exact conditions used in these studies are not known by the author, and the heat transfer within the flotation bag could conceivably differ from the value calculated using the experimental correlation. An analysis was performed in which the amount of heat transfer within the analysis was increased while leaving the other operating parameters unchanged. The results of this analysis indicated that the heat-transfer rate could be increased by a factor of 100 without creating a sufficient loss of buoyancy to cause the loss of the vehicle. This is a result of the increase in buoyancy due to the expansion of the gas as the vehicle rises dominating over the loss of buoyancy due to heat-transfer effects. Thus, it is apparent that, even with a significant amount of inaccuracies in the heat-transfer portion of this analysis, the recovery system is shown to be adequate to return the test vehicle to the surface.

A second quantity not known with certainty is the terminal velocity of the test vehicle as it is rising towards the surface. A detailed discussion of this quantity and its effect on the successful surface arrival of the vehicle will be presented in a later section of this report. However because this quantity is not known with the certainty of other parameters within this analysis, it was treated as a variable in a sensitivity analysis. Vertical velocities larger than the 5 ft/s used as the nominal value are not a problem from a buoyancy standpoint because, although the forced convection heat transfer on the outside of the flotation bag would be enhanced, the amount of time for the loss of buoyancy to occur is significantly reduced. The expansion of the gas as the vehicle rises rapidly dominates over heat-transfer effects, and thus the higher velocities reduce the chance of losing the vehicle due to loss of buoyancy effects. Velocities less than the nominal 5 ft/s increase the amount of time during which heat transfer can occur and could conceivably result in the loss of the vehicle. In the sensitivity analysis, drag coefficients were increased, resulting in terminal velocities as low as 1 ft/s. In each case, the loss of buoyancy due to heat transfer was insufficient to result in the loss of the vehicle. Velocities lower than 1 ft/s are not considered realistic, and thus it is apparent that variations in terminal velocity cannot result in loss of buoyancy and the subsequent loss of the vehicle due to heat-transfer effects.

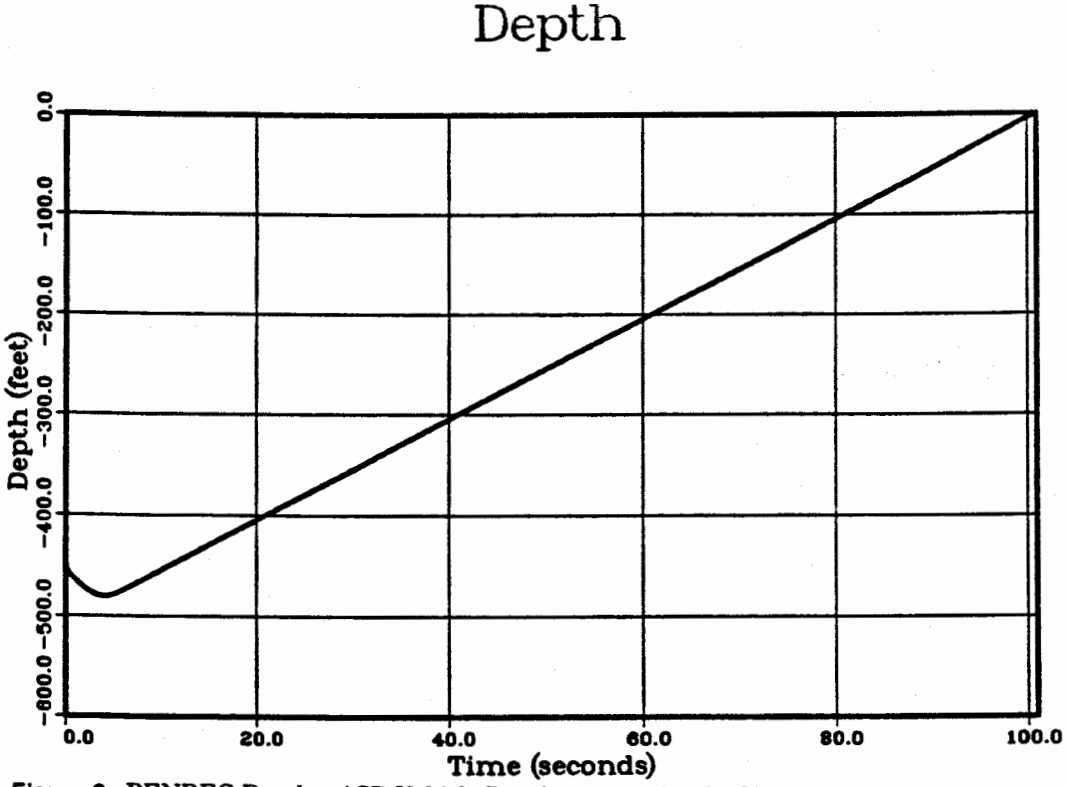

Figure 3. PENREC Results: ASP Vehicle Depth History for the Nominal Case

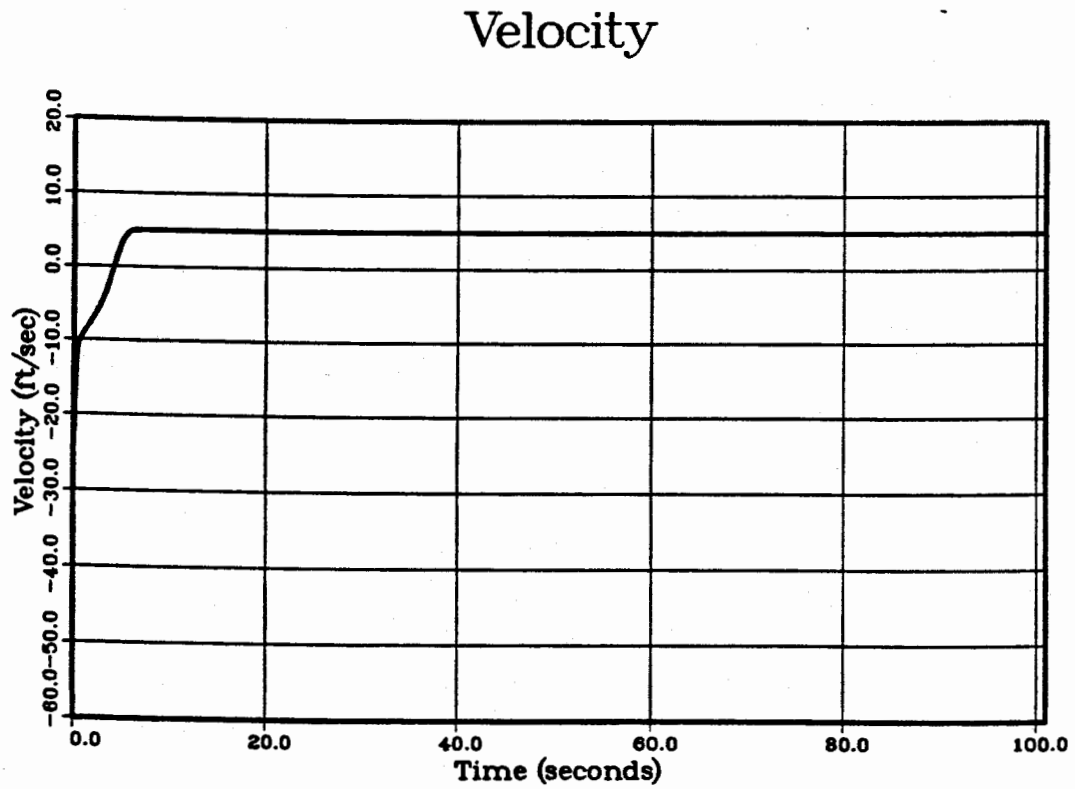

Figure 4. PENREC Results: ASP Vehicle Velocity History for the Nominal Case

The operating performance of the gas generator used in this analysis is based upon both the results of experiments and theoretical predictions performed by RRC. Experiments conducted at Sandia National Laboratories in Albuquerque, in which the gas generator was operated into a closed vessel, indicated that the device performed better than the prediction that was used in this analysis. Thus, the buoyancy provided by the gas generator should be more than sufficient to recover the ASP vehicle from the 450 ft nominal depth. However, the possibility of a gas generator malfunction does exist, and a sensitivity analysis was performed to determine what factor of safety exists in the amount of buoyancy provided by the flotation system. In this analysis, the buoyancy generated during the fill process was decreased by a constant factor, resulting in a partially full flotation bag at the end of the fill process. It was found that the gas generator system could produce as little as 83% of the predicted buoyancy without resulting in the loss of the vehicle. This fact, in conjunction with the results of Sandia's test of the gas generator system, indicates that the gas generator has a sufficient factor of safety, and slight errors in its predicted performance should not result in the loss of the vehicle.

The deployment system is activated by a timing mechanism initiated at water impact. A pitch-over during water entry, or a higher sink rate than anticipated, could conceivably result in the recovery system being activated at a depth in excess of the 450-ft design depth. To determine the maximum possible deployment depth, a sensitivity analysis was performed in which the initial depth in the analysis was increased until a loss-of-buoyancy situation developed. The analysis predicts that the recovery system can successfully recover the ASP vehicle to depths of 582 ft. At depths slightly greater than this value, the vehicle begins to rise, but the heat transfer results in a loss of buoyancy and the subsequent loss of the vehicle. The accuracy of this maximum operating depth is certainly subject to the limitations of the analysis, but this value is sufficient to provide guidelines for the timer settings should recovery from depths greater than the design depth be desired in future flights.

3. Surface Arrival Analysis

Solution Technique

The solution technique for the surface-arrival analysis is very similar to the technique used to analyze the recovery system. The effects of heat transfer are not considered significant, and thus the analysis is considerably less complex than the recovery system analysis. The calculations are initiated with the vehicle at a depth of 10 ft rising at a terminal velocity with the flotation bag fully inflated. The most significant difference in the governing equations is that the buoyant force caused by the flotation gas is limited to the force caused by that quantity of gas below the surface of the water. Thus, as the flotation bag breaks the surface, the buoyancy is decreased accordingly.

The analysis of the surface-arrival process has been written in the form of the FORTRAN computer program PENSUR (PENetrator SURface analysis). A listing of this program is included in Appendix C of this report. Figure 7 is a flow chart of this program that outlines the major steps in the analysis. The first step in the analysis, like the recovery system analysis, is to define physical constants and set the initial conditions. The headings for the output are then written, and the calculation loop is initiated. The initial step within the analysis loop is the calculation of the gas properties at the present depth. These properties include pressure, temperature, density, and volume. The gas buoyant force is then calculated based only upon that portion of the flotation gas below the surface of the water. The drag force is then calculated based upon a constant drag coefficient, and the sum of the forces acting on the penetrator is then used to determine the vehicle's acceleration. From this value of the acceleration, the velocity and depth at the new time are calculated. The results are then written, the variables are reset, a check is made to determine if the analysis has reached a preset time limit, and if not, the analysis returns to the beginning of the analysis loop. If the time limit has been reached, the analysis is terminated.

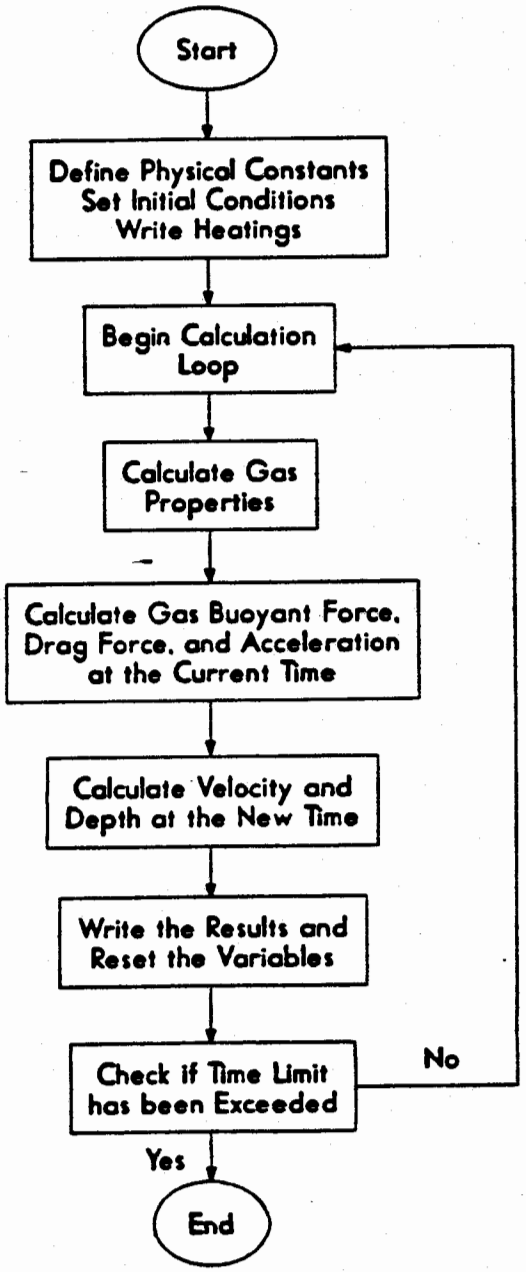

Figure 7. Flow Chart for the Program PENSUR

Analysis Results

The initial purpose of this analysis was to determine the cause of the sinking of the test vehicle in the Lake Pend Oreille test, which was discussed briefly in the introduction. In this test, the vehicle reached a terminal velocity of approximately 10 ft/s during the ascent. Upon reaching the surface, the vehicle rose to a point at which a significant fraction of the flotation bag was above the surface, and then sank to the end of a safety line attached to the vehicle's nose. When the vehicle was returned to the surface with the safety line, it was found to be positively buoyant.

The surface-arrival analysis was used to predict the performance of the vehicle with a terminal velocity of 10 ft/s. Figure 8 is a plot of the predicted depth as a function of time, and Figure 9 is a plot of the predicted net buoyant force of the ASP vehicle and the recovery system as a function of time. The depth plotted in Figure 8 is measured from the junction of the flotation bag and the ASP vehicle to the surface. The dotted line represents the depth at which the top of the flotation bag reaches the surface. Thus, when the depth line is above the dotted line in this figure, part of the flotation bag is exposed above the water surface. It can be seen in this figure that the analysis predicts the loss of the vehicle, similar to what occurred in the experiment.

The reason the vehicle sank can be seen in the plot of the net buoyancy, Figure 9. Initially the vehicle had a net buoyancy of 168.3 lbf, which corresponds to a full flotation bag. As the vehicle is rising, the gas is expanding due to the decrease in hydrostatic pressure, and vents out at the bottom of the bag. The bag is constructed with a vent at the base to prevent the gas pressure from exceeding the local hydrostatic pressure. When the vehicle reaches the surface at a time between 0.2 and 0.3 s, the buoyancy falls due to the bag rising above the surface. The gas continues to expand and vent out of the bottom of the bag until the minimum depth is reached and the vehicle's velocity reaches zero. At this point the vehicle has a negative net buoyancy because inertial effects have carried it above its neutrally buoyant point. The vehicle then begins to settle down into the water, with the net buoyancy rising as the bag continues to submerge. The bag becomes completely submerged at a time of approximately 1.8 s after the start of the analysis. The net buoyancy at this point is only 94.4 lbf due to the compression of the gas as the depth of the bag vent increases. This amount of buoyancy is not sufficient to arrest the downward motion of the vehicle before further compression of the gas causes the net buoyancy to drop below zero at a time of approximately 3.9 s. Thus, the vehicle continues to sink. The amount of gas in the bag is constant from the point at which the vehicle reaches its minimum depth, and thus when it was brought to the surface with the line in the experiment, sufficient buoyancy existed to allow it to float.

The results of the Lake Pend Oreille test and this analysis indicated that the vehicle was lost due to excessive terminal velocities during the ascent, which caused the vehicle to lose an excessive amount of buoyancy as the top of the flotation bag rose above the surface. Thus, the remaining amount of buoyancy was insufficient to stop the resulting downward motion of the vehicle. To decrease the terminal velocity of the vehicle, an inverted parachute was designed and attached to the bottom of the flotation bag to increase the drag of the recovery system and thus decrease the terminal velocity. This parachute was designed to provide enough drag to slow the vehicle to approximately 5 ft/s at maximum buoyancy conditions. A series of PENSUR runs with different drag coefficients indicated that a terminal velocity of less than approximately 9 ft/s is necessary to ensure a successful surface arrival. Figures 10 and 11 are plots of depth and net buoyant force for a terminal velocity of 5 ft/s. A copy of the PENSUR output for this case is included as Appendix D. In this case, the vertical velocity is sufficiently low such that the top of the bag remains above the surface as the vehicle oscillates about the neutral buoyancy point. A second test conducted at Lake Pend Oreille with the inverted parachute attached to the flotation bag resulted in the successful recovery of the vehicle.

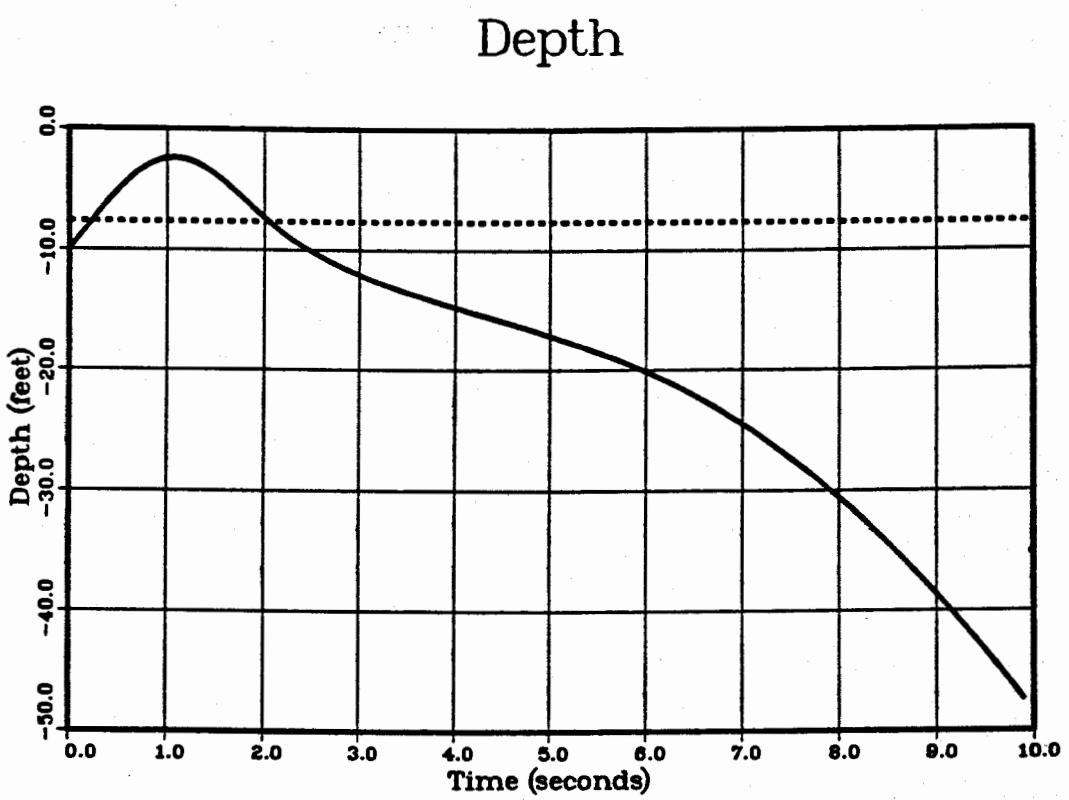

Figure 8. PENSUR Results: ASP Vehicle Depth History for the 10 ft/s Terminal Velocity Case

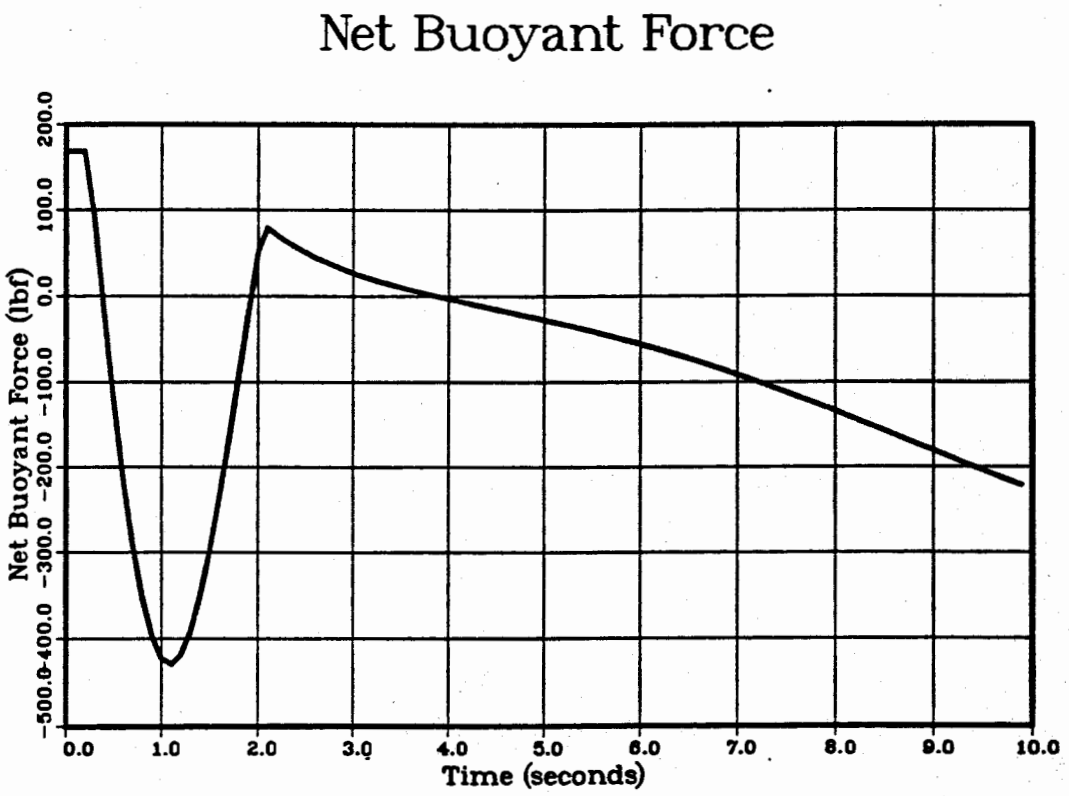

Figure 9. PENSUR Results: ASP Vehicle Net Buoyant Force History for the 10 ft/s Terminal Velocity Case

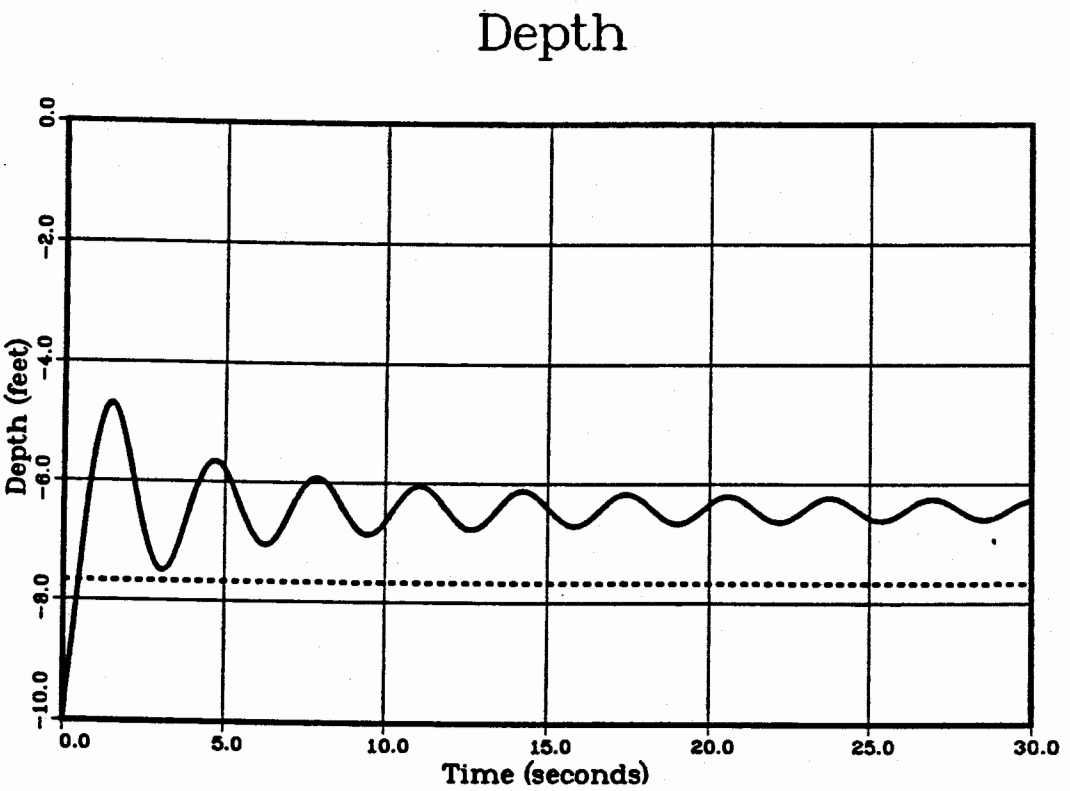

Figure 10. PENSUR Results: ASP Vehicle Depth History for the 5 ft/s Terminal Velocity Case

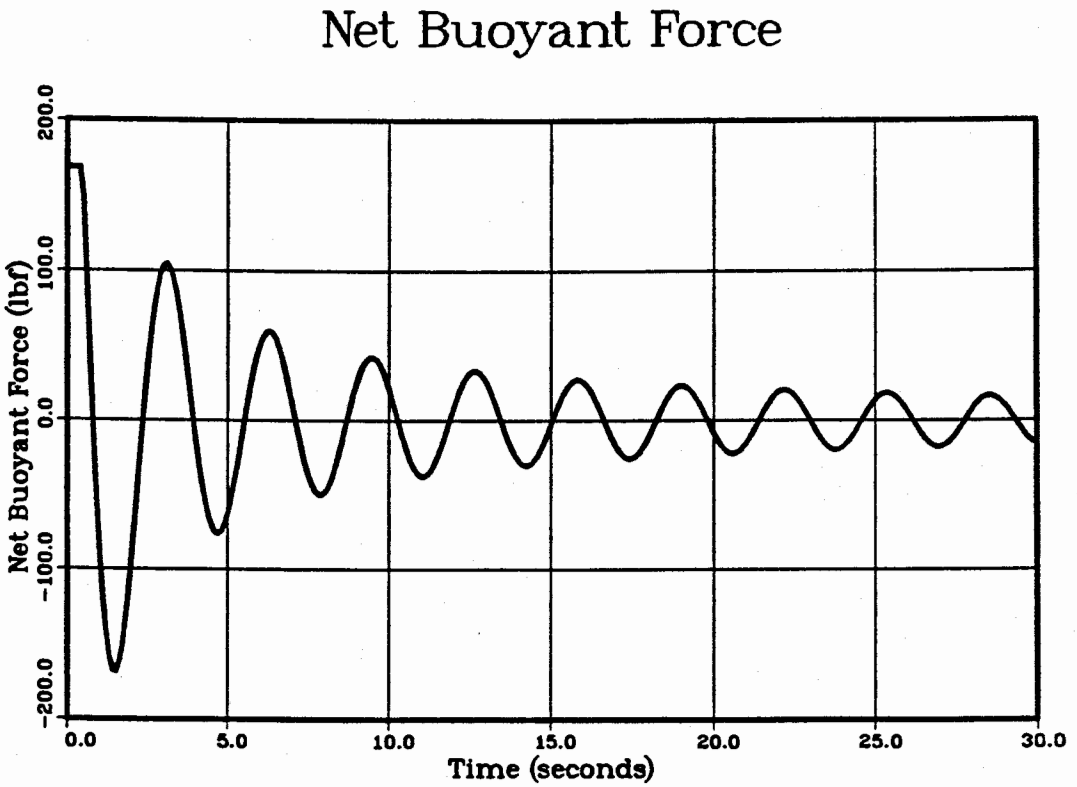

Figure 11. PENSUR Results: ASP Vehicle Net Buoyant Force History for the 5 ft/s Terminal Velocity Case

4. Conclusions

The analyses described in this report have been used to predict the performance of the ASP vehicle during the recovery portion of the test flight. The performance of the recovery system during deployment and ascent has been modeled with the program PENREC. The results of this model indicate that the effects of heat transfer on the gas buoyancy are not significant, and loss of the vehicle due to cooling of the gas in the nominal case is not possible. In addition to resolving the heat-transfer issue, this analysis has been used to estimate safe operating limits of the recovery system, including maximum deployment depth and minimum gas generator performance. The surface arrival analysis, written in the form of the program PENSUR, has been used to explain the loss of the vehicle during the first test of the recovery system, and to estimate the necessary reduction in terminal velocity to ensure successful recovery of the vehicle.

Reference

[1]J. P. Holman, *Heat Transfer, Third Edition (New York: McGraw-Hill Book Company, 1972) p. 224.*

APPENDIX A

Program PENREC Listing

```
      PROGRAM PENREC
C
C ... THIS PROGRAM CALCULATES THE TIME HISTORY OF THE
C ...  PENETRATOR RECOVERY SYSTEM FROM INITIAL CONDITIONS
C ...  AT A PREDETERMINED DEPTH TO FLOTATION AT THE SURFACE.
C
      REAL MUF,KF,NUFNC,MG,MUG,KG,MUW,KW,LPEN,NUFC,KB
C
      OPEN(UNIT=7,FILE='PENREC.OUT',STATUS='NEW')
C
C ... DEFINE PHYSICAL CONSTANTS
C
      PI=3.1415926
      G=32.174
      GC=32.174
      RECRIT=5.E5
      PATM=14.696*144.
C
C ... SET INITIAL CONDITIONS
C
      NWC=0
      IFLAG=0
      TIME=0.
      DELTAT=0.01
      DB=1.5
      TB=40.+460.
      HB=92./12.
      LPEN=65.443/12.
      DEPTH=-450.
      RHOW=64.1
      P600=(600.*RHOW*G/GC)+PATM
      VEL=-60.
      CD=3.824
      CDCHUTE=7.
      WGHT=803.
      BFPEN=138.
      BFG=0.
      VOLG=0.
      BFGMAX=833.3
      VOLGMAX=(BFGMAX/RHOW)*GC/G
      TG600=227.+460.
      TG=TG600
      PG=(-1.*DEPTH*RHOW*G/GC)+PATM
      RG=35.12
      GAMMAG=1.30
C
C ... WRITE HEADINGS
C
      WRITE(7,903)
  903 FORMAT(5X,'PENREC RESULTS')
      WRITE(7,904)
  904 FORMAT(///,10X,'TIME',6X,'DEPTH',5X,'VELOCITY',4X,'VOL.-G',
     $4X,'TEMP.-G',4X,'TEMP.-B',4X,'TEMP.-W',
     $5X,'B.F.-G',
```

```
     $6X,'D.F.',7X,'Q-DOT',2X,'N',/)
C
C ... BEGIN CALCULATION LOOP
C
  100 IF(DEPTH.GE.0..OR.DEPTH.LT.-800.)GO TO 900
C
C ... CALCULATE PROPERTIES DURING BAG-FILL
C
      IF(TIME.LT.6.)THEN
C
C ... CALCULATE DRAG FORCE, ACCELERATION, AND NEW VELOCITY AND DEPTH
C
        DF=-0.5*CD*(PI*(DB/2.)**2)*RHOW*ABS(VEL)*VEL/GC
        IF(VEL.LT.0.)DF=-0.5*CDCHUTE*RHOW*ABS(VEL)*VEL/GC
C
        DVDT=(-1.*WGHT+BFG+BFPEN+DF)/(WGHT/G)
C
        VEL2=VEL+DELTAT*DVDT
C
        DEPTH2=DEPTH+((VEL+VEL2)/2.)*DELTAT
C
C ... CALCULATE GAS BUOYANT FORCE FOR BAG FILL AT 600 FT. DEPTH
C
         IF(TIME.LE.0.4)BGF2600=0.
         IF(TIME.GT.0.4.AND.TIME.LE.3.7)
     $   BFG2600=196.13*(TIME+DELTAT)-721.13+642.
         IF(TIME.GT.3.7.AND.TIME.LE.6.)
     $   BFG2600=36.09*(TIME+DELTAT)-133.53+642.
C
C ... CALCULATE GAS BUOYANT FORCE AT NEW DEPTH
C
        PG2=(-1.*DEPTH2*RHOW*G/GC)+PATM
        BFG2=BFG2600*(PG2/P600)**(-1./GAMMAG)
        IF(BFG2.GT.BFGMAX)BFG2=BFGMAX
        TG2=TG600*(PG2/P600)**((GAMMAG-1.)/GAMMAG)
        VOLG2=(BFG2/RHOW)*GC/G
        TW=((DEPTH2+600.)/600.)*(70.-40.)+40.+460.
        IF(TW.LT.500.)TW=500.
        TB=TW
C
        GO TO 800
C
      ENDIF
C
C ... CALCULATE WATER PROPERTIES
C
      TW=((DEPTH+600.)/600.)*(70.-40.)+40.+460.
      IF(TW.LT.500.)TW=500.
      MUW=(TW-500.)*(-3.933E-7)+3.23E-5
      KW=(TW-500.)*(2.037E-7)+9.028E-5
      PRW=(TW-500.)*(-0.1593)+11.6
      CPW=PRW*KW/(MUW*GC)
C
C ... CALCULATE GAS BAG PROPERTIES
```

```
C
      HG=(VOLG-(((DB/2.)**3)*4.*PI/6.))/(PI*(DB/2.)**2)
      AG=PI*DB*HG+2.*PI*(DB/2)**2
C
C ... CALCULATE GAS PROPERTIES
C
      RHOG=PG/(RG*TG)
      MG=RHOG*VOLG
C
      MUG=2.861E-7*((491.6+400.)/(TG+400.))*(TG/491.6)**1.5
      KG=2.335E-6*((491.6+4000.)/(TG+4000.))*(TG/491.6)**1.5
      PRG=0.76
      CPG=PRG*KG/(MUG*GC)
C
C ... CALCULATE REYNOLDS NUMBER
C
      IF(VEL.LT.0.)RE=RHOW*ABS(VEL)*(LPEN+HB)/(MUW*GC)
      IF(VEL.GE.0.)RE=RHOW*VEL*HG/(MUW*GC)
C
      NFLAG=0
C
C ... BEGIN HEAT TRANSFER LOOP
C
      DO 1 N=1,20
C
C ... CALCULATE GAS PROPERTIES AT THE FILM TEMPERATURE
C
      TF=0.5*(TB+TG)
      RHOF=PG/(RG*TF)
      MUF=2.861E-7*((491.6+400.)/(TF+400.))*(TF/491.6)**1.5
      KF=2.335E-6*((491.6+4000.)/(TF+4000.))*(TF/491.6)**1.5
      PRF=0.76
      CPF=PRF*KF/(MUF*GC)
C
C ... CALCULATE NATURAL CONVECTION HEAT TRANSFER (BAG TO GAS)
C
      GRF=(G*ABS(TG-TB)*(HG**3)*(RHOF**2))/(GC*GC*TF*(MUF**2))
      NUFNC=0.55*(GRF*PRF)**0.25
      HNC=NUFNC*KF/DB
C
      QDOT=HNC*AG*(TB-TG)
C
C ... CALCULATE FORCED CONVECTION HEAT TRANSFER (WATER TO BAG)
C
      IF(RE.LT.RECRIT)THEN
        IF(VEL.GT.0.)THEN
        NUFC=0.664*(PRW**0.333)*(RE**0.5)
        ELSE
        RELPENB=RE*(LPEN+HB-HG)/(LPEN+HB)
        NUFC=0.664*(PRW**0.333)*((RE**0.5)-(RELPENB**0.5))
        ENDIF
      ELSE
        IF(VEL.GT.0.)THEN
        NUFC=(PRW**0.333)*(0.036*(RE**0.8)-836.)
```

```
            ELSE
            RELPENB=RE*(LPEN+HB-HG)/(LPEN+HB)
            NUFC=0.036*(PRW**0.333)*((RE**0.8)-(RELPENB**0.8))
            ENDIF
          ENDIF
C
          HFC=NUFC*KW/HG
C
C ... CHECK FOR CONVERGENCE IN BAG TEMPERATURE
C
          TB2=-1.*(QDOT/(HFC*AG)-TW)
C
          TPROD=(TG-TB)*(TB-TW)
          IF(TPROD.LT.0..AND.TG.GT.TW)TB2=TW+0.2
          IF(TPROD.LT.0..AND.TG.LT.TW)TB2=TW-0.2
C
          DELTB=ABS(TB2-TB)
C
          IF(NFLAG.EQ.1)GO TO 2
C
          IF(DELTB.LE.0.1)NFLAG=1
C
          TB=(TB+TB2)/2.
C
        1 CONTINUE
C
        2 CONTINUE
C
C ... CALCULATE THE DRAG FORCE, ACCELERATION, AND NEW VELOCITY AND DEI
C
          DF=-0.5*CD*(PI*(DB/2.)**2)*RHOW*ABS(VEL)*VEL/GC
          IF(VEL.LT.0.)DF=-0.5*CDCHUTE*RHOW*ABS(VEL)*VEL/GC
C
          DVDT=(-1.*WGHT+BFG+BFPEN+DF)/(WGHT/G)
C
          VEL2=VEL+DELTAT*DVDT
C
          DEPTH2=DEPTH+((VEL+VEL2)/2.)*DELTAT
C
C ... CALCULATE NEW GAS TEMPERATURE DUE TO BOTH HEAT TRANSFER
C ...  AND COMPRESSION
C
          TG1A=(QDOT*DELTAT/(MG*CPG))+TG
C
          PG2=(-1.*RHOW*DEPTH2*G/GC)+PATM
          TG2=TG1A*(PG2/PG)**((GAMMAG-1.)/GAMMAG)
C
          VOLG2=MG*RG*TG2/PG2
          IF(VOLG2.GT.VOLGMAX)MG=(PG2*VOLGMAX)/(RG*TG2)
          IF(VOLG2.GT.VOLGMAX)VOLG2=VOLGMAX
C
C ... CALCULATE THE NEW BUOYANT FORCE
C
          BFG2=RHOW*VOLG2*G/GC
```

```
C
  800 CONTINUE
C
C ... WRITE THE RESULTS AT 0.1 SECOND INTERVALS
C
      IF(NWC.EQ.0.OR.NWC.EQ.10)THEN
       WRITE(7,901)TIME,DEPTH,VEL,VOLG,TG,TB,TW,BFG,DF,QDOT,N
  901  FORMAT(5X,F9.2,2X,9(F10.3,1X),I2)
       NWC=0
      ENDIF
      NWC=NWC+1
C
C ... RESET THE VARIABLES
C
      TIME=TIME+DELTAT
      DEPTH=DEPTH2
      VEL=VEL2
      BFG=BFG2
      VOLG=VOLG2
      TG=TG2
      PG=PG2
C
      GO TO 100
C
  900 CONTINUE
C
C ... DETERMINE AND WRITE SURFACE TIME
C
      IF(DEPTH.GT.0.)THEN
      TSUR=(-1.*DEPTH/VEL)+TIME
      WRITE(6,902)TSUR
      WRITE(7,902)TSUR
  902 FORMAT(//,5X,'PROGRAM PREDICTS SURFACE ARRIVAL AT ',F8.2,
     $' SECONDS.')
      ENDIF
C
C ... WRITE LOSS OF VEHICLE MESSAGE
C
      IF(DEPTH.LT.-600.)THEN
      WRITE(6,905)
      WRITE(7,905)
  905 FORMAT(//,5X,'PROGRAM PREDICTS LOSS OF VEHICLE.')
      ENDIF
C
      STOP
      END
```

APPENDIX B

Program PENREC Sample Output

This appendix includes an abbreviated sample output of the program PENREC. This output is in the form of a table, with the columns containing the following variables:

Column 1: Time (seconds)

Column 2: Depth (ft)

Column 3: Velocity (ft/s)

Column 4: Gas Volume (ft^3)

Column 5: Gas Temperature (°R)

Column 6: Bag Temperature (°R)

Column 7: Water Temperature (°R)

Column 8: Gas Buoyant Force (lbf)

Column 9: Drag Force (lbf)

Column 10: Heat Transfer Rate (Btu/s)

Column 11: Number of Iterations within the Heat Transfer Loop

The first two pages of the complete output are included in this Appendix to provide details of the bag fill and the recovery system performance through the time at which the vehicle reaches the terminal vertical velocity. The last page of the output is included to provide details of the recovery system at the time of surface arrival. The output pages during the terminal velocity portion of the ascent are not included because they provide little additional information.

5.40	-477.256	4.271	12.952	653.663	506.139	506.139	830.207	-122.816	0.000	0
5.50	-476.820	4.432	13.000	653.534	506.161	506.161	833.300	-132.209	0.000	0
5.60	-476.370	4.562	13.000	653.401	506.184	506.184	833.300	-140.071	0.000	0
5.70	-475.909	4.663	13.000	653.264	506.207	506.207	833.300	-146.361	0.000	0
5.80	-475.439	4.741	13.000	653.125	506.230	506.230	833.300	-151.333	0.000	0
5.90	-474.961	4.802	13.000	652.983	506.254	506.254	833.300	-155.229	0.000	0
6.00	-474.479	4.849	13.000	652.840	510.125	506.276	833.300	-158.260	-14.097	8
6.10	-473.992	4.885	13.000	652.348	510.128	506.300	833.300	-160.605	-14.028	2
6.20	-473.502	4.912	13.000	651.857	510.112	506.325	833.300	-162.413	-13.962	2
6.30	-473.010	4.933	13.000	651.367	510.101	506.350	833.300	-163.802	-13.895	2
6.40	-472.516	4.949	13.000	650.877	510.095	506.374	833.300	-164.867	-13.828	2
6.50	-472.020	4.961	13.000	650.389	510.091	506.399	833.300	-165.682	-13.761	2
6.60	-471.524	4.970	13.000	649.902	510.090	506.424	833.300	-166.304	-13.693	2
6.70	-471.026	4.978	13.000	649.416	510.091	506.449	833.300	-166.780	-13.626	2
6.80	-470.528	4.983	13.000	648.930	510.093	506.474	833.300	-167.142	-13.559	2
6.90	-470.030	4.987	13.000	648.447	510.096	506.499	833.300	-167.418	-13.492	2
7.00	-469.531	4.990	13.000	647.964	510.100	506.523	833.300	-167.629	-13.425	2
7.10	-469.032	4.993	13.000	647.483	510.104	506.548	833.300	-167.789	-13.358	2
7.20	-468.532	4.994	13.000	647.004	510.109	506.573	833.300	-167.911	-13.292	2
7.30	-468.033	4.996	13.000	646.525	510.115	506.598	833.300	-168.004	-13.226	2
7.40	-467.533	4.997	13.000	646.048	510.121	506.623	833.300	-168.075	-13.160	2
7.50	-467.034	4.998	13.000	645.573	510.127	506.648	833.300	-168.129	-13.094	2
7.60	-466.534	4.998	13.000	645.099	510.133	506.673	833.300	-168.170	-13.029	2
7.70	-466.034	4.999	13.000	644.626	510.139	506.698	833.300	-168.201	-12.963	2
7.80	-465.534	4.999	13.000	644.154	510.146	506.723	833.300	-168.225	-12.899	2
7.90	-465.034	4.999	13.000	643.684	510.153	506.748	833.300	-168.243	-12.834	2
8.00	-464.534	5.000	13.000	643.216	510.160	506.773	833.300	-168.256	-12.770	2
8.10	-464.034	5.000	13.000	642.749	510.167	506.798	833.300	-168.267	-12.705	2
8.20	-463.534	5.000	13.000	642.282	510.174	506.823	833.300	-168.275	-12.642	2
8.30	-463.034	5.000	13.000	641.818	510.181	506.848	833.300	-168.281	-12.578	2
8.40	-462.535	5.000	13.000	641.354	510.188	506.873	833.300	-168.285	-12.515	2
8.50	-462.035	5.000	13.000	640.893	510.196	506.898	833.300	-168.289	-12.452	2
8.60	-461.535	5.000	13.000	640.432	510.203	506.923	833.300	-168.292	-12.389	2
8.70	-461.035	5.000	13.000	639.972	510.211	506.948	833.300	-168.294	-12.326	2
8.80	-460.535	5.000	13.000	639.514	510.218	506.973	833.300	-168.295	-12.264	2
8.90	-460.035	5.000	13.000	639.058	510.226	506.998	833.300	-168.296	-12.202	2
9.00	-459.535	5.000	13.000	638.602	510.234	507.023	833.300	-168.297	-12.140	2
9.10	-459.035	5.000	13.000	638.148	510.242	507.048	833.300	-168.298	-12.079	2
9.20	-458.536	5.000	13.000	637.696	510.250	507.073	833.300	-168.298	-12.017	2
9.30	-458.036	5.000	13.000	637.245	510.258	507.098	833.300	-168.299	-11.956	2
9.40	-457.536	5.000	13.000	636.794	510.266	507.123	833.300	-168.299	-11.896	2
9.50	-457.036	5.000	13.000	636.345	510.274	507.148	833.300	-168.299	-11.835	2
9.60	-456.536	5.000	13.000	635.898	510.282	507.173	833.300	-168.299	-11.775	2
9.70	-456.036	5.000	13.000	635.452	510.291	507.198	833.300	-168.299	-11.715	2
9.80	-455.536	5.000	13.000	635.006	510.299	507.223	833.300	-168.299	-11.655	2
9.90	-455.036	5.000	13.000	634.563	510.308	507.248	833.300	-168.299	-11.596	2
10.00	-454.537	5.000	13.000	634.120	510.316	507.273	833.300	-168.299	-11.536	2
10.10	-454.037	5.000	13.000	633.679	510.325	507.298	833.300	-168.299	-11.477	2
10.20	-453.537	5.000	13.000	633.239	510.334	507.323	833.300	-168.299	-11.419	2
10.30	-453.037	5.000	13.000	632.800	510.342	507.348	833.300	-168.299	-11.360	2
10.40	-452.537	5.000	13.000	632.363	510.351	507.373	833.300	-168.299	-11.302	2
10.50	-452.037	5.000	13.000	631.927	510.360	507.398	833.300	-168.299	-11.244	2
10.60	-451.537	5.000	13.000	631.492	510.369	507.423	833.300	-168.299	-11.186	2
10.70	-451.037	5.000	13.000	631.058	510.378	507.448	833.300	-168.299	-11.129	2
10.80	-450.538	5.000	13.000	630.625	510.387	507.473	833.300	-168.299	-11.071	2
10.90	-450.038	5.000	13.000	630.194	510.397	507.498	833.300	-168.299	-11.014	2
11.00	-449.538	5.000	13.000	629.764	510.406	507.523	833.300	-168.299	-10.957	2
11.10	-449.038	5.000	13.000	629.335	510.415	507.548	833.300	-168.299	-10.901	2
11.20	-448.538	5.000	13.000	628.907	510.425	507.573	833.300	-168.299	-10.844	2
11.30	-448.038	5.000	13.000	628.480	510.434	507.598	833.300	-168.299	-10.788	2

95.40	-27.571	5.000	13.000	425.713	527.972	528.621	833.300	-168.299	3.166 2
95.50	-27.071	5.000	13.000	425.409	527.997	528.646	833.300	-168.299	3.165 2
95.60	-26.571	5.000	13.000	425.102	528.023	528.671	833.300	-168.299	3.165 2
95.70	-26.071	5.000	13.000	424.793	528.048	528.696	833.300	-168.299	3.164 2
95.80	-25.571	5.000	13.000	424.481	528.073	528.721	833.300	-168.299	3.163 2
95.90	-25.071	5.000	13.000	424.167	528.099	528.746	833.300	-168.299	3.163 2
96.00	-24.571	5.000	13.000	423.851	528.124	528.771	833.300	-168.299	3.162 2
96.10	-24.071	5.000	13.000	423.532	528.150	528.796	833.300	-168.299	3.161 2
96.20	-23.571	5.000	13.000	423.211	528.175	528.821	833.300	-168.299	3.160 2
96.30	-23.071	5.000	13.000	422.887	528.200	528.846	833.300	-168.299	3.099 2
96.40	-22.571	5.000	13.000	422.560	528.226	528.871	833.300	-168.299	3.098 2
96.50	-22.071	5.000	13.000	422.231	528.251	528.896	833.300	-168.299	3.097 2
96.60	-21.571	5.000	13.000	421.899	528.277	528.921	833.300	-168.299	3.095 2
96.70	-21.071	5.000	13.000	421.564	528.302	528.946	833.300	-168.299	3.094 2
96.80	-20.571	5.000	13.000	421.226	528.328	528.971	833.300	-168.299	3.093 2
96.90	-20.071	5.000	13.000	420.885	528.353	528.996	833.300	-168.299	3.091 2
97.00	-19.571	5.000	13.000	420.541	528.379	529.021	833.300	-168.299	3.090 2
97.10	-19.071	5.000	13.000	420.194	528.404	529.046	833.300	-168.299	3.088 2
97.20	-18.571	5.000	13.000	419.844	528.430	529.071	833.300	-168.299	3.086 2
97.30	-18.071	5.000	13.000	419.491	528.455	529.096	833.300	-168.299	3.085 2
97.40	-17.571	5.000	13.000	419.134	528.481	529.121	833.300	-168.299	3.083 2
97.50	-17.071	5.000	13.000	418.774	528.506	529.146	833.300	-168.299	3.081 2
97.60	-16.571	5.000	13.000	418.410	528.532	529.171	833.300	-168.299	3.079 2
97.70	-16.071	5.000	13.000	418.043	528.558	529.196	833.300	-168.299	3.077 2
97.80	-15.571	5.000	13.000	417.672	528.583	529.221	833.300	-168.299	3.075 2
97.90	-15.071	5.000	13.000	417.298	528.609	529.246	833.300	-168.299	3.072 2
98.00	-14.571	5.000	13.000	416.919	528.635	529.271	833.300	-168.299	3.070 2
98.10	-14.071	5.000	13.000	416.537	528.660	529.296	833.300	-168.299	3.068 2
98.20	-13.571	5.000	13.000	416.151	528.686	529.321	833.300	-168.299	3.065 2
98.30	-13.071	5.000	13.000	415.761	528.712	529.346	833.300	-168.299	3.062 2
98.40	-12.571	5.000	13.000	415.367	528.737	529.371	833.300	-168.299	3.060 2
98.50	-12.071	5.000	13.000	414.968	528.763	529.396	833.300	-168.299	3.057 2
98.60	-11.571	5.000	13.000	414.565	528.789	529.421	833.300	-168.299	3.054 2
98.70	-11.071	5.000	13.000	414.157	528.815	529.446	833.300	-168.299	3.051 2
98.80	-10.571	5.000	13.000	413.744	528.841	529.471	833.300	-168.299	3.048 2
98.90	-10.071	5.000	13.000	413.327	528.867	529.496	833.300	-168.299	3.045 2
99.00	-9.571	5.000	13.000	412.905	528.892	529.521	833.300	-168.299	3.042 2
99.10	-9.071	5.000	13.000	412.478	528.918	529.546	833.300	-168.299	3.038 2
99.20	-8.571	5.000	13.000	412.046	528.944	529.571	833.300	-168.299	3.035 2
99.30	-8.071	5.000	13.000	411.609	528.970	529.596	833.300	-168.299	3.031 2
99.40	-7.571	5.000	13.000	411.166	528.996	529.621	833.300	-168.299	3.028 2
99.50	-7.071	5.000	13.000	410.717	529.022	529.646	833.300	-168.299	3.024 2
99.60	-6.571	5.000	13.000	410.263	529.048	529.671	833.300	-168.299	3.020 2
99.70	-6.071	5.000	13.000	409.803	529.074	529.696	833.300	-168.299	3.016 2
99.80	-5.571	5.000	13.000	409.337	529.100	529.721	833.300	-168.299	3.012 2
99.90	-5.071	5.000	13.000	408.865	529.126	529.746	833.300	-168.299	3.008 2
100.00	-4.571	5.000	13.000	408.386	529.152	529.771	833.300	-168.299	3.003 2
100.10	-4.071	5.000	13.000	407.900	529.178	529.796	833.300	-168.299	2.999 2
100.20	-3.571	5.000	13.000	407.408	529.204	529.821	833.300	-168.299	2.994 2
100.30	-3.070	5.000	13.000	406.909	529.231	529.846	833.300	-168.299	2.989 2
100.40	-2.570	5.000	13.000	406.402	529.257	529.871	833.300	-168.299	2.985 2
100.50	-2.070	5.000	13.000	405.888	529.283	529.896	833.300	-168.299	2.980 2
100.60	-1.570	5.000	13.000	405.367	529.309	529.922	833.300	-168.299	2.974 2
100.70	-1.070	5.000	13.000	404.837	529.335	529.946	833.300	-168.299	2.969 2
100.80	-0.570	5.000	13.000	404.300	529.362	529.971	833.300	-168.299	2.964 2
100.90	-0.070	5.000	13.000	403.753	529.388	529.996	833.300	-168.299	2.958 2

PROGRAM PREDICTS SURFACE ARRIVAL AT 100.92 SECONDS.

APPENDIX C

Program PENSUR Listing

```
      PROGRAM PENSUR
C
C ... THIS PROGRAM CALCULATES THE TIME HISTORY OF THE
C ...  PENETRATOR RECOVERY SYSTEM DURING SURFACE ARRIVAL.
C
      REAL MUF,KF,NUFNC,MG,MUG,KG,MUW,KW,LPEN,NUFC,KB
C
      OPEN(UNIT=7,FILE='PENSUR.OUT',STATUS='NEW')
C
C ... DEFINE PHYSICAL CONSTANTS
C
      PI=3.1415926
      G=32.174
      GC=32.174
      PATM=14.696*144.
C
C ... SET INITIAL CONDITIONS
C
      NWC=0
      TIME=0.
      DELTAT=0.01
      TIMEL=30.*DELTAT
      RG=35.12
      GAMMAG=1.30
      DB=1.5
      LPEN=65.443/12.
      HB=92./12.
      RHOW=64.1
      CD=3.824
      WGHT=803.
      BFPEN=138.
      BFGMAX=833.3
      VOLGMAX=(BFGMAX/RHOW)*GC/G
      DEPTH=-10.
      PG0=((-1.*RHOW*DEPTH)*G/GC)+PATM
      TG=404.
      MG=(PG0*VOLGMAX)/(RG*TG)
      VEL=SQRT((BFGMAX+BFPEN-WGHT)*GC/
     $(0.5*CD*PI*RHOW*(DB/2.)**2))
C
C ... WRITE HEADINGS
C
      WRITE(7,903)
  903 FORMAT(5X,'PENSUR RESULTS')
      WRITE(7,904)
  904 FORMAT(///,10X,'TIME',6X,'DEPTH',5X,'VELOCITY',5X,
     $'MASS-G',4X,'VOL.-G',
     $4X,'TEMP.-G',4X,'B.F.-G',5X,'B.F.-N'6X,'D.F.',/)
C
C ... BEGIN CALCULATION LOOP
C
 1000 CONTINUE
C
C ... CALCULATE GAS PROPERTIES
```

APPENDIX D

Program PENSUR Sample Output

This appendix includes a sample output of the program PENREC. This output is in the form of a table, with the columns containing the following variables:

Column 1: Time (seconds)

Column 2: Depth (ft)

Column 3: Velocity (ft/s)

Column 4: Gas Mass (lbm)

Column 5: Gas Volume (ft^3)

Column 6: Gas Temperature (°R)

Column 7: Gas Buoyant Force (lbf)

Column 8: Net Buoyant Force (lbf)

Column 9: Drag Force (lbf)

PENSUR RESULTS

TIME	DEPTH	VELOCITY	MASS-G	VOL.-G	TEMP.-G	B.F.-G	B.F.-N	D.F.
0.00	-10.000	5.000	2.526	13.000	404.000	833.300	168.300	-168.300
0.10	-9.500	5.000	2.504	13.000	402.911	833.300	168.300	-168.300
0.20	-9.000	5.000	2.481	13.000	401.813	833.300	168.300	-168.300
0.30	-8.500	5.000	2.458	13.000	400.704	833.300	168.300	-168.300
0.40	-8.000	5.000	2.435	13.000	399.585	833.300	168.300	-168.300
0.50	-7.500	4.991	2.413	13.000	398.456	814.420	149.420	-167.697
0.60	-7.007	4.832	2.390	13.000	397.332	758.613	93.613	-157.159
0.70	-6.539	4.514	2.368	13.000	396.254	705.555	40.555	-137.167
0.80	-6.108	4.082	2.349	13.000	395.255	656.782	-8.218	-112.139
0.90	-5.725	3.567	2.331	13.000	394.358	613.399	-51.601	-85.644
1.00	-5.397	2.994	2.316	13.000	393.584	576.194	-88.806	-60.347
1.10	-5.128	2.381	2.303	13.000	392.946	545.722	-119.278	-38.149
1.20	-4.922	1.739	2.294	13.000	392.455	522.368	-142.632	-20.357
1.30	-4.781	1.079	2.287	13.000	392.118	506.394	-158.606	-7.839
1.40	-4.706	0.409	2.284	13.000	391.940	497.962	-167.038	-1.124
1.50	-4.699	-0.266	2.283	12.999	391.923	497.064	-167.936	0.475
1.60	-4.759	-0.921	2.283	12.983	392.066	502.810	-162.190	5.707
1.70	-4.881	-1.512	2.283	12.951	392.358	514.600	-150.400	15.390
1.80	-5.058	-2.003	2.283	12.904	392.780	531.650	-133.350	27.008
1.90	-5.278	-2.372	2.283	12.847	393.302	552.892	-112.108	37.867
2.00	-5.528	-2.611	2.283	12.783	393.893	577.118	-87.882	45.880
2.10	-5.796	-2.724	2.283	12.715	394.523	603.092	-61.908	49.943
2.20	-6.069	-2.723	2.283	12.647	395.162	629.654	-35.346	49.900
2.30	-6.337	-2.622	2.283	12.580	395.786	655.761	-9.239	46.294
2.40	-6.590	-2.439	2.283	12.518	396.373	680.523	15.523	40.054
2.50	-6.822	-2.189	2.283	12.462	396.908	703.195	38.195	32.246
2.60	-7.026	-1.884	2.283	12.413	397.376	723.175	58.175	23.905
2.70	-7.198	-1.539	2.283	12.373	397.768	739.986	74.986	15.939
2.80	-7.333	-1.162	2.283	12.341	398.076	753.262	88.262	9.091
2.90	-7.430	-0.764	2.283	12.318	398.296	762.734	97.734	3.926
3.00	-7.485	-0.351	2.283	12.305	398.423	768.221	103.221	0.831
3.10	-7.500	0.067	2.283	12.302	398.455	769.620	104.620	-0.030
3.20	-7.472	0.481	2.283	12.308	398.392	766.915	101.915	-1.555
3.30	-7.404	0.866	2.283	12.324	398.239	760.265	95.265	-5.052
3.40	-7.301	1.202	2.283	12.348	398.002	750.060	85.060	-9.730
3.50	-7.166	1.472	2.283	12.380	397.696	736.880	71.880	-14.592
3.60	-7.009	1.667	2.283	12.418	397.335	721.430	56.430	-18.702
3.70	-6.835	1.782	2.283	12.459	396.938	704.479	39.479	-21.386
3.80	-6.655	1.821	2.283	12.503	396.522	686.800	21.800	-22.319
3.90	-6.474	1.788	2.283	12.547	396.103	669.122	4.122	-21.513
4.00	-6.299	1.691	2.283	12.590	395.699	652.109	-12.891	-19.242
4.10	-6.137	1.539	2.283	12.630	395.322	636.337	-28.663	-15.938
4.20	-5.993	1.341	2.283	12.666	394.986	622.292	-42.708	-12.103
4.30	-5.870	1.106	2.283	12.696	394.699	610.372	-54.628	-8.235
4.40	-5.773	0.843	2.283	12.721	394.470	600.887	-64.113	-4.780
4.50	-5.703	0.559	2.283	12.739	394.305	594.072	-70.928	-2.100
4.60	-5.662	0.261	2.283	12.749	394.208	590.087	-74.913	-0.459
4.70	-5.651	-0.043	2.283	12.752	394.183	589.025	-75.975	0.012
4.80	-5.670	-0.343	2.283	12.747	394.228	590.905	-74.095	0.794
4.90	-5.719	-0.626	2.283	12.735	394.343	595.632	-69.368	2.642
5.00	-5.794	-0.877	2.283	12.716	394.520	602.962	-62.038	5.177
5.10	-5.893	-1.083	2.283	12.691	394.751	612.524	-52.476	7.900
5.20	-6.009	-1.237	2.283	12.662	395.023	623.851	-41.149	10.308
5.30	-6.138	-1.335	2.283	12.630	395.324	636.417	-28.583	12.004

5.40	-6.274	-1.376	2.283	12.596	395.641	649.670	-15.330	12.752
5.50	-6.412	-1.363	2.283	12.562	395.960	663.067	-1.933	12.499
5.60	-6.545	-1.298	2.283	12.529	396.269	676.093	11.093	11.348
5.70	-6.670	-1.189	2.283	12.499	396.557	688.279	23.279	9.521
5.80	-6.782	-1.042	2.283	12.472	396.814	699.215	34.215	7.303
5.90	-6.877	-0.862	2.283	12.449	397.034	708.552	43.552	5.002
6.00	-6.953	-0.657	2.283	12.431	397.209	716.007	51.007	2.908
6.10	-7.008	-0.434	2.283	12.418	397.334	721.364	56.364	1.268
6.20	-7.040	-0.199	2.283	12.410	397.407	724.471	59.471	0.266
6.30	-7.047	0.042	2.283	12.408	397.424	725.240	60.240	-0.012
6.40	-7.031	0.281	2.283	12.412	397.387	723.653	58.653	-0.530
6.50	-6.992	0.505	2.283	12.422	397.297	719.787	54.787	-1.719
6.60	-6.931	0.705	2.283	12.436	397.158	713.836	48.836	-3.346
6.70	-6.852	0.871	2.283	12.455	396.976	706.093	41.093	-5.103
6.80	-6.758	0.996	2.283	12.478	396.761	696.928	31.928	-6.675
6.90	-6.654	1.077	2.283	12.503	396.521	686.760	21.760	-7.804
7.00	-6.544	1.112	2.283	12.530	396.267	676.031	11.031	-8.327
7.10	-6.433	1.103	2.283	12.557	396.010	665.182	0.182	-8.197
7.20	-6.325	1.053	2.283	12.583	395.759	654.632	-10.368	-7.469
7.30	-6.224	0.966	2.283	12.608	395.524	644.764	-20.236	-6.279
7.40	-6.133	0.846	2.283	12.631	395.313	635.917	-29.083	-4.816
7.50	-6.056	0.699	2.283	12.650	395.132	628.381	-36.619	-3.286
7.60	-5.994	0.530	2.283	12.665	394.988	622.389	-42.611	-1.891
7.70	-5.950	0.346	2.283	12.676	394.886	618.121	-46.879	-0.804
7.80	-5.925	0.151	2.283	12.683	394.827	615.703	-49.297	-0.153
7.90	-5.920	-0.048	2.283	12.684	394.815	615.203	-49.797	0.016
8.00	-5.935	-0.245	2.283	12.680	394.850	616.637	-48.363	0.405
8.10	-5.969	-0.431	2.283	12.672	394.929	619.938	-45.062	1.249
8.20	-6.020	-0.596	2.283	12.659	395.050	624.950	-40.050	2.390
8.30	-6.087	-0.733	2.283	12.642	395.205	631.441	-33.559	3.619
8.40	-6.166	-0.838	2.283	12.623	395.389	639.116	-25.884	4.723
8.50	-6.253	-0.906	2.283	12.601	395.593	647.638	-17.362	5.522
8.60	-6.346	-0.936	2.283	12.578	395.807	656.647	-8.353	5.900
8.70	-6.439	-0.930	2.283	12.555	396.024	665.776	0.776	5.816
8.80	-6.531	-0.888	2.283	12.533	396.235	674.673	9.673	5.305
8.90	-6.616	-0.814	2.283	12.512	396.432	683.008	18.008	4.459
9.00	-6.692	-0.712	2.283	12.494	396.609	690.485	25.485	3.412
9.10	-6.757	-0.586	2.283	12.478	396.759	696.849	31.849	2.314
9.20	-6.809	-0.442	2.283	12.466	396.877	701.890	36.890	1.313
9.30	-6.845	-0.283	2.283	12.457	396.961	705.445	40.445	0.540
9.40	-6.865	-0.116	2.283	12.452	397.007	707.403	42.403	0.090
9.50	-6.868	0.055	2.283	12.451	397.014	707.700	42.700	-0.021
9.60	-6.854	0.224	2.283	12.455	396.981	706.329	41.329	-0.337
9.70	-6.824	0.382	2.283	12.462	396.912	703.351	38.351	-0.983
9.80	-6.779	0.523	2.283	12.473	396.807	698.907	33.907	-1.840
9.90	-6.720	0.640	2.283	12.487	396.673	693.200	28.200	-2.755
10.00	-6.652	0.728	2.283	12.504	396.514	686.489	21.489	-3.571
10.10	-6.576	0.786	2.283	12.522	396.339	679.066	14.066	-4.157
10.20	-6.495	0.811	2.283	12.542	396.154	671.243	6.243	-4.427
10.30	-6.414	0.804	2.283	12.561	395.966	663.338	-1.662	-4.351
10.40	-6.336	0.766	2.283	12.581	395.784	655.656	-9.344	-3.955
10.50	-6.262	0.701	2.283	12.599	395.613	648.481	-16.519	-3.309
10.60	-6.196	0.611	2.283	12.615	395.460	642.069	-22.931	-2.515
10.70	-6.140	0.501	2.283	12.629	395.330	636.639	-28.361	-1.687
10.80	-6.097	0.374	2.283	12.640	395.228	632.373	-32.627	-0.939
10.90	-6.066	0.234	2.283	12.647	395.157	629.406	-35.594	-0.370
11.00	-6.050	0.088	2.283	12.651	395.119	627.836	-37.164	-0.052
11.10	-6.049	-0.062	2.283	12.652	395.116	627.711	-37.289	0.026
11.20	-6.062	-0.209	2.283	12.648	395.148	629.035	-35.965	0.294
11.30	-6.090	-0.347	2.283	12.641	395.213	631.749	-33.251	0.809

11.40	-6.131	-0.469	2.283	12.631	395.308	635.732	-29.268	1.479
11.50	-6.183	-0.570	2.283	12.618	395.430	640.807	-24.193	2.186
11.60	-6.244	-0.646	2.283	12.603	395.572	646.753	-18.247	2.813
11.70	-6.312	-0.696	2.283	12.587	395.728	653.317	-11.683	3.258
11.80	-6.383	-0.717	2.283	12.569	395.893	660.226	-4.774	3.457
11.90	-6.454	-0.709	2.283	12.552	396.058	667.205	2.205	3.387
12.00	-6.523	-0.675	2.283	12.535	396.219	673.983	8.983	3.068
12.10	-6.588	-0.616	2.283	12.519	396.368	680.307	15.307	2.555
12.20	-6.646	-0.535	2.283	12.505	396.502	685.948	20.948	1.928
12.30	-6.695	-0.436	2.283	12.493	396.614	690.707	25.707	1.279
12.40	-6.733	-0.322	2.283	12.484	396.701	694.421	29.421	0.697
12.50	-6.759	-0.197	2.283	12.478	396.761	696.964	31.964	0.261
12.60	-6.772	-0.066	2.283	12.475	396.792	698.251	33.251	0.029
12.70	-6.772	0.068	2.283	12.475	396.791	698.239	33.239	-0.031
12.80	-6.758	0.199	2.283	12.478	396.760	696.928	31.928	-0.266
12.90	-6.732	0.321	2.283	12.484	396.700	694.378	29.378	-0.693
13.00	-6.695	0.429	2.283	12.493	396.614	690.701	25.701	-1.236
13.10	-6.647	0.517	2.283	12.505	396.504	686.061	21.061	-1.802
13.20	-6.592	0.584	2.283	12.518	396.377	680.661	15.661	-2.297
13.30	-6.531	0.626	2.283	12.533	396.236	674.729	9.729	-2.642
13.40	-6.467	0.643	2.283	12.548	396.089	668.510	3.510	-2.786
13.50	-6.403	0.635	2.283	12.564	395.940	662.253	-2.747	-2.714
13.60	-6.341	0.603	2.283	12.579	395.796	656.199	-8.801	-2.444
13.70	-6.284	0.548	2.283	12.594	395.662	650.574	-14.426	-2.021
13.80	-6.232	0.474	2.283	12.606	395.543	645.582	-19.418	-1.510
13.90	-6.189	0.383	2.283	12.617	395.443	641.398	-23.602	-0.987
14.00	-6.156	0.279	2.283	12.625	395.366	638.166	-26.834	-0.524
14.10	-6.134	0.166	2.283	12.631	395.314	635.993	-29.007	-0.185
14.20	-6.123	0.047	2.283	12.633	395.289	634.954	-30.046	-0.015
14.30	-6.125	-0.074	2.283	12.633	395.292	635.084	-29.916	0.036
14.40	-6.138	-0.191	2.283	12.630	395.323	636.376	-28.624	0.246
14.50	-6.162	-0.300	2.283	12.623	395.381	638.776	-26.224	0.606
14.60	-6.197	-0.396	2.283	12.615	395.462	642.178	-22.822	1.056
14.70	-6.241	-0.475	2.283	12.604	395.564	646.438	-18.562	1.519
14.80	-6.292	-0.534	2.283	12.592	395.681	651.371	-13.629	1.919
14.90	-6.347	-0.571	2.283	12.578	395.810	656.774	-8.226	2.192
15.00	-6.405	-0.584	2.283	12.564	395.944	662.426	-2.574	2.299
15.10	-6.463	-0.575	2.283	12.549	396.079	668.102	3.102	2.228
15.20	-6.519	-0.544	2.283	12.536	396.209	673.585	8.585	1.995
15.30	-6.571	-0.493	2.283	12.523	396.329	678.667	13.667	1.638
15.40	-6.617	-0.424	2.283	12.512	396.436	683.162	18.162	1.212
15.50	-6.656	-0.340	2.283	12.503	396.524	686.910	21.910	0.780
15.60	-6.685	-0.245	2.283	12.495	396.592	689.779	24.779	0.403
15.70	-6.704	-0.141	2.283	12.491	396.636	691.669	26.669	0.133
15.80	-6.713	-0.032	2.283	12.489	396.656	692.514	27.514	0.007
15.90	-6.711	0.078	2.283	12.489	396.651	692.285	27.285	-0.041
16.00	-6.698	0.185	2.283	12.492	396.620	690.991	25.991	-0.231
16.10	-6.674	0.284	2.283	12.498	396.566	688.688	23.688	-0.544
16.20	-6.641	0.371	2.283	12.506	396.490	685.476	20.476	-0.925
16.30	-6.600	0.441	2.283	12.516	396.396	681.494	16.494	-1.311
16.40	-6.553	0.494	2.283	12.527	396.288	676.913	11.913	-1.640
16.50	-6.502	0.525	2.283	12.540	396.170	671.921	6.921	-1.858
16.60	-6.449	0.536	2.283	12.553	396.046	666.724	1.724	-1.935
16.70	-6.396	0.526	2.283	12.566	395.923	661.526	-3.474	-1.862
16.80	-6.345	0.496	2.283	12.579	395.804	656.528	-8.472	-1.655
16.90	-6.297	0.447	2.283	12.590	395.694	651.916	-13.084	-1.347
17.00	-6.256	0.383	2.283	12.600	395.597	647.860	-17.140	-0.985
17.10	-6.221	0.304	2.283	12.609	395.517	644.504	-20.496	-0.623
17.20	-6.195	0.215	2.283	12.615	395.457	641.965	-23.035	-0.312
17.30	-6.178	0.119	2.283	12.620	395.418	640.332	-24.668	-0.095

17.40	-6.172	0.018	2.283	12.621	395.402	639.660	-25.340	-0.002
17.50	-6.175	-0.083	2.283	12.620	395.409	639.974	-25.026	0.046
17.60	-6.188	-0.181	2.283	12.617	395.440	641.261	-23.739	0.219
17.70	-6.211	-0.271	2.283	12.612	395.493	643.466	-21.534	0.493
17.80	-6.242	-0.349	2.283	12.604	395.565	646.497	-18.503	0.821
17.90	-6.280	-0.413	2.283	12.594	395.654	650.223	-14.777	1.148
18.00	-6.324	-0.459	2.283	12.584	395.755	654.490	-10.510	1.421
18.10	-6.371	-0.487	2.283	12.572	395.866	659.121	-5.879	1.598
18.20	-6.421	-0.496	2.283	12.560	395.980	663.931	-1.069	1.653
18.30	-6.470	-0.485	2.283	12.548	396.094	668.729	3.729	1.581
18.40	-6.517	-0.455	2.283	12.536	396.203	673.332	8.332	1.395
18.50	-6.560	-0.409	2.283	12.526	396.303	677.565	12.565	1.126
18.60	-6.598	-0.348	2.283	12.517	396.391	681.273	16.273	0.814
18.70	-6.629	-0.274	2.283	12.509	396.463	684.320	19.320	0.506
18.80	-6.653	-0.191	2.283	12.503	396.517	686.599	21.599	0.245
18.90	-6.667	-0.101	2.283	12.500	396.550	688.029	23.029	0.068
19.00	-6.673	-0.007	2.283	12.498	396.563	688.558	23.558	0.000
19.10	-6.669	0.087	2.283	12.499	396.554	688.169	23.169	-0.051
19.20	-6.655	0.177	2.283	12.503	396.523	686.875	21.875	-0.211
19.30	-6.634	0.260	2.283	12.508	396.473	684.732	19.732	-0.455
19.40	-6.604	0.332	2.283	12.515	396.404	681.832	16.832	-0.740
19.50	-6.568	0.389	2.283	12.524	396.320	678.299	13.299	-1.021
19.60	-6.527	0.431	2.283	12.534	396.225	674.279	9.279	-1.251
19.70	-6.482	0.455	2.283	12.545	396.123	669.939	4.939	-1.394
19.80	-6.436	0.461	2.283	12.556	396.016	665.453	0.453	-1.432
19.90	-6.390	0.449	2.283	12.567	395.910	660.997	-4.003	-1.359
20.00	-6.347	0.420	2.283	12.578	395.809	656.743	-8.257	-1.189
20.10	-6.307	0.376	2.283	12.588	395.716	652.851	-12.149	-0.950
20.20	-6.272	0.317	2.283	12.596	395.636	649.462	-15.538	-0.678
20.30	-6.244	0.248	2.283	12.603	395.570	646.701	-18.299	-0.413
20.40	-6.223	0.169	2.283	12.609	395.521	644.663	-20.337	-0.193
20.50	-6.210	0.085	2.283	12.612	395.492	643.422	-21.578	-0.048
20.60	-6.206	-0.003	2.283	12.613	395.482	643.021	-21.979	0.000
20.70	-6.211	-0.090	2.283	12.612	395.493	643.476	-21.524	0.055
20.80	-6.224	-0.174	2.283	12.608	395.524	644.767	-20.233	0.204
20.90	-6.245	-0.250	2.283	12.603	395.573	646.842	-18.158	0.422
21.00	-6.274	-0.316	2.283	12.596	395.639	649.612	-15.388	0.673
21.10	-6.308	-0.369	2.283	12.588	395.719	652.962	-12.038	0.916
21.20	-6.347	-0.406	2.283	12.578	395.809	656.753	-8.247	1.111
21.30	-6.389	-0.427	2.283	12.568	395.906	660.832	-4.168	1.229
21.40	-6.432	-0.431	2.283	12.557	396.006	665.035	0.035	1.253
21.50	-6.474	-0.419	2.283	12.547	396.105	669.198	4.198	1.181
21.60	-6.515	-0.390	2.283	12.537	396.199	673.160	8.160	1.026
21.70	-6.552	-0.347	2.283	12.528	396.284	676.773	11.773	0.812
21.80	-6.584	-0.291	2.283	12.520	396.358	679.901	14.901	0.572
21.90	-6.610	-0.225	2.283	12.514	396.418	682.432	17.432	0.341
22.00	-6.629	-0.151	2.283	12.509	396.462	684.274	19.274	0.153
22.10	-6.640	-0.071	2.283	12.506	396.487	685.359	20.359	0.034
22.20	-6.643	0.012	2.283	12.506	396.494	685.650	20.650	-0.001
22.30	-6.638	0.094	2.283	12.507	396.482	685.135	20.135	-0.059
22.40	-6.624	0.172	2.283	12.510	396.451	683.835	18.835	-0.198
22.50	-6.604	0.243	2.283	12.515	396.403	681.804	16.804	-0.396
22.60	-6.576	0.303	2.283	12.522	396.340	679.129	14.129	-0.619
22.70	-6.543	0.351	2.283	12.530	396.264	675.921	10.921	-0.831
22.80	-6.506	0.385	2.283	12.539	396.179	672.313	7.313	-0.998
22.90	-6.467	0.403	2.283	12.549	396.087	668.452	3.452	-1.095
23.00	-6.426	0.406	2.283	12.558	395.993	664.493	-0.507	-1.107
23.10	-6.386	0.392	2.283	12.568	395.901	660.589	-4.411	-1.035
23.20	-6.348	0.364	2.283	12.578	395.813	656.892	-8.108	-0.891
23.30	-6.314	0.322	2.283	12.586	395.733	653.539	-11.461	-0.697

29.40	-6.412	0.328	2.283	12.562	395.961	663.121	-1.879	-0.723
29.50	-6.380	0.312	2.283	12.570	395.887	659.993	-5.007	-0.654
29.60	-6.356	0.284	2.283	12.577	395.818	657.081	-7.919	-0.542
29.70	-6.324	0.245	2.283	12.584	395.756	654.493	-10.507	-0.465
29.80	-6.301	0.198	2.283	12.589	395.704	652.326	-12.674	-0.263
29.90	-6.284	0.143	2.283	12.593	395.665	650.659	-14.341	-0.138
30.00	-6.273	0.083	2.283	12.596	395.638	649.554	-15.446	-0.046

INTERNAL DISTRIBUTION ONLY:

1510 J. W. Nunziato
1530 L. W. Davison
1540 W. C. Luth
1550 R. C. Maydew
1551 J. K. Cole
1551 C. E. Hailey
1551 W. P. Wolfe
1552 C. W. Peterson
1552 D. W. Johnson
1552 D. E. Waye
1553 S. McAlees, Jr. (5)
1553 D. W. Kuntz (10)
1554 D. D. McBride
1555 W. R. Barton
1555 L. R. Rollstin
1556 W. L. Oberkampf
8100 E. E. Ives
Attn: J. B. Wright, 8150
8152 J. C. Swearengen
8152 R. N. Everett
8152 M. T. Ferrario
8152 R. E. Rychnovsky
8301 W. R. Bolton
8462 H. D. Sorensen
8024 P. W. Dean
3141 S. A. Landenberger (5)
3141 W. L. Garner

~~3241~~

[redacted]

M0659 G. R. Schreiner, DOE/AL, OIEA